

Innovation-triggered Learning with Application to Data-driven Predictive Control

Kaikai Zheng, Dawei Shi, Sandra Hirche, and Yang Shi

Abstract—Data-driven control has attracted lots of attention in recent years, especially for plants that are difficult to model based on first principles. In particular, a key issue in data-driven approaches is how to make efficient use of data as the abundance of data becomes overwhelming. To address this issue, this work proposes an innovation-triggered learning framework and a corresponding data-driven controller design approach with guaranteed stability. Specifically, we consider a linear time-invariant system with unknown dynamics. A set-membership approach is introduced to learn a parametric uncertainty set for the unknown dynamics. Then, a data selection mechanism is proposed by online evaluating the innovation contained in the sampled data, wherein the innovation is quantified by its effect of shrinking the parametric uncertainty set. Next, after introducing a stability criterion using the set-membership estimate of the system dynamics, a robust data-driven predictive controller is designed by minimizing a worst-case cost function. The closed-loop stability of the data-driven predictive controller equipped with the innovation-triggered learning protocol is discussed within a high probability framework. Finally, comparative numerical experiments are performed to verify the validity of the proposed approach, and the characteristics and the design principle of the learning hyper-parameter are also discussed.

Index Terms—Innovation-triggered learning; Set-membership learning; Data-driven predictive control; High-probability stability.

I. INTRODUCTION

Recent developments in advanced sensing and communication technology are offering an increasing volume of data for control systems design, which accelerates the advancements on the methodological front of data-driven control [1]–[6]. Among others, data efficiency is an important issue that needs to be addressed as the abundance of data becomes overwhelming in control systems. In this work, we aim to introduce a solution by online selecting the data that contains new information of the system dynamics within a set-membership framework, and integrating the data selection scheme with data-driven predictive control.

K. Zheng and D. Shi are with the MIIT Key Laboratory of Servo Motion System Drive and Control, School of Automation, Beijing Institute of Technology, Beijing 100081, China (e-mail: kaikai.zheng@bit.edu.cn, dawei.shi@bit.edu.cn).

S. Hirche is with the Chair of Information-oriented Control, Technical University of Munich, Barer Strasse 21, 80333, Munich, Germany (e-mail: hirche@tum.de).

Y. Shi is with the Department of Mechanical Engineering, Faculty of Engineering, University of Victoria, Victoria, BC V8N 3P6, Canada (e-mail: yshi@uvic.ca).

Set-membership learning methods offer a systematic framework to learn system dynamics and evaluate the learning performance [7]–[9]. This approach was first proposed for linear systems to deal with performance evaluation problems of finite-sample learning methods. For linear systems with Gaussian noise, the authors in [10] proposed a set-membership learning method to estimate a credibility region of unknown parameters. Similarly, an uncertainty set was learned in [11] to bound the error in parameter estimation procedures used in the design of a robust controller. An admissible set of system parameters was obtained as quadratic matrix inequality (QMI) for linear systems with bounded noise in [3], [12]. Set-membership learning methods have also been proven useful in learning nonlinear systems. A set-membership approach was used in [13] to analyze the boundedness of the error for the estimated nonlinear models. The authors in [14] proposed a relaxed-greedy learning method for nonlinear systems, whose performance was further analyzed using a set-membership approach. Later in [15], an algorithm was developed for experiment design using set-membership learning to minimize the radius of information. For other methods of set-membership learning, the interested readers can refer to [16]–[18] and references therein.

The focus of this work is also closely related to data-driven predictive control (DPC), which features the adoption of a data-driven prediction model in the constrained optimization problem solved to obtain the controller output at each sampling instant. Several DPC methods have been proposed in the literature by exploiting the advantages of different data-driven models [19]–[25]. Based on the renowned fundamental lemma [26], a Data-Enabled Predictive Control (DeePC) was first proposed for linear systems [27] and then generalized to various types of settings, including noise-corrupted data [28], [29], nonlinear systems [30], [31], online learning and control [32], [33]. Gaussian processes were also employed in the design of DPC [34], [35]. For instance, the DPC in [34] was proposed by learning the additive nonlinear model mismatch using a Gaussian process. In addition, set-membership models were also explored for data-driven predictive controller [36], [37]. A set of candidate plant models was learned at each time step in [36], based on which a predictive controller was designed to enforce input and output constraints for all the plants within the learned model set. In [37], an online set-membership system identification approach combined with homothetic prediction tubes was used to ensure robust constraint satisfaction in the designed predictive control. However, with the accumulation of incoming data during the operation of

the control system, an important question to answer is when to update the prediction model for improved data efficiency (and the consequently reduced computation complexity) while guaranteeing control performance.

Event-triggered learning (ETL) provides an effective remedy to overcome this issue by learning only when certain pre-specified conditions are violated [38], [39]. ETL can improve computational efficiency by reducing the complexity of non-parametric models or by decreasing the updating frequency of parametric models. For non-parametric models, more available data usually leads to an enlarged computational burden, which can be alleviated using ETL by learning from selected data samples [40], [41]. Specifically, for Gaussian processes, data samples were selected according to a model uncertainty criterion [42]–[44] or an associated entropy-based criterion [38]. For parametric models, although the complexity of the model does not change with the amount of training data, the frequent model updates would lead to increased computational burden. Several ETL approaches were thus proposed for parametric models by identifying the change in system dynamics and adjusting the model only when necessary [45]. For instance, for linear systems with intermittent communication processes, the authors in [39] proposed two learning mechanisms triggered by the distribution and expectation of inter-communication time, respectively. For finite impulse response models, event-triggered parameter identification approaches were proposed for binary-valued observations [46] and quantized observations [47]. Despite the advances in ETL, it is still unclear how to quantify and evaluate the importance of the incoming data samples online in a data-driven fashion by exploiting the structural properties of the underlying system dynamics, which motivates the investigation in this work.

In this paper, the objective is to introduce a systematic data selection method and a learning-based control approach with theoretically guaranteed performance. Specifically, we consider a linear time-invariant (LTI) system with unknown dynamics and disturbances, and the selected dataset is updated in an *innovation-triggered* fashion. Here, the innovation of a data sample (or innovativeness) is quantified by its effect of shrinking the set of potential dynamics compatible with data samples. We consider the scenario that only limited prior knowledge of the disturbance is available, which is characterized with a form of generic concentration inequality. A few challenges, however, need to be addressed to enable the design of the innovation-triggered learning (ITL) protocol and the corresponding data-driven controller. First, the effect of the unknown disturbance with the adopted prior knowledge blurs the characteristics of the system dynamics, which makes it more challenging to ensure the learning and control performance. Second, since the innovation of a data sample depends on the unknown system dynamics and the data recorded previously, it is challenging to design an online data selection protocol that identifies a slim dataset to support a learning algorithm with ensured theoretical properties. In addition, the inferred system dynamics in this work are represented using a set-membership method and are updated intermittently, which adds to the difficulties in the design of the data-driven predictive controller and the corresponding

stability analysis. The main contributions of this work are summarized as follows:

- 1) Compared with the existing literature that considered bounded deterministic disturbance [3] or Gaussian disturbance [10], a set-membership learning method for linear systems is proposed in the form of a QMI for disturbances modeled by a generic concentration inequality. A matrix parameter is further designed for the set-membership learning method, which ensures that the learned parametric uncertainty set contains the unknown parameters with a high probability.
- 2) Utilizing the proposed set-membership learning method, an ITL mechanism is introduced by quantifying the innovation of new data samples. Specifically, the innovation of a data sample is characterized in terms of its effect of shrinking the set of system dynamics compatible with the sampled data. It is proved that, with a predefined probability, the Lebesgue measure of the learned parametric uncertainty set decreases exponentially under the ITL mechanism. The special cases of bounded deterministic disturbances and stochastic disturbances with covariance information are discussed.
- 3) The applicability of the ITL approach to data-driven predictive control is demonstrated. To do this, a data-driven predictive controller is introduced within a min-max optimization framework based on the proposed ITL schemes. The proposed control approach features the design of a robust data-driven predictive controller that intermittently updates its prediction model only when the incoming data can help reduce the uncertainty of the learned system dynamics. The closed-loop stability is theoretically guaranteed in the sense of high probability by designing a data-based linear matrix inequality (LMI).

The remainder of this paper is organized as follows. Section II presents the main problem considered in our work, useful definitions and lemmas are also introduced. The main theoretical results on set-membership learning, ITL, and their application to data-driven predictive control are presented in Section III. Moreover, implementation issues, numerical verification, and comparison results are comprehensively presented in Section IV, followed by the concluding remarks in Section V.

Notation. In this work, $\text{diag}\{x_1, \dots, x_n\}$ represents a diagonal matrix with diagonal elements being $\{x_1, \dots, x_n\}$, and I_n represents an n -dimensional identity matrix. For matrices A and B , $A \succ B$ and $A \succeq B$ denote that matrix $A - B$ is positive definite and positive semi-definite, respectively. Moreover, $A \not\succeq B$ denotes that the matrix $B - A$ is not a positive semi-definite matrix. For a random variable, $\mathbb{P}[\cdot]$ and $\mathbb{E}[\cdot]$ represent the probability and the expectation, respectively. The eigenvalues of a matrix $A \in \mathbb{R}^{n \times n}$ are written as $\lambda(A) = [\lambda_1(A), \lambda_2(A), \dots, \lambda_n(A)]$ with $|\lambda_1(A)| \geq |\lambda_2(A)| \geq \dots \geq |\lambda_n(A)|$, and the Moore-Penrose inverse of A is denoted as A^\dagger . The cardinality of a set \mathcal{D} is denoted as $\|\mathcal{D}\|$. Moreover, $|A|$ and $\text{Tr}(A)$ denote the determinant and the trace of matrix A , respectively.

II. PROBLEM FORMULATION

Consider a linear time-invariant system

$$\mathbf{x}(k+1) = A_* \mathbf{x}(k) + B_* \mathbf{u}(k) + \mathbf{w}(k), \quad (1)$$

where $\mathbf{x}(k) \in \mathbb{R}^{n_x \times 1}$ is the state, $\mathbf{u}(k) \in \mathbb{R}^{n_u \times 1}$ is the input, $\mathbf{w}(k)$ is the disturbance, and $A_* \in \mathbb{R}^{n_x \times n_x}$, $B_* \in \mathbb{R}^{n_x \times n_u}$ are unknown system parameters.

The data samples collected up to time step k are represented as $\mathcal{D}(k)$, and the index set of the dataset is denoted as $\mathcal{R}(k)$. Therefore, the dataset $\mathcal{D}(k)$ can be expressed as:

$$\begin{aligned} \mathcal{D}(k) &:= \{(\mathbf{x}(i), \mathbf{u}(i), \mathbf{x}(i+1)) | i \in \mathcal{R}(k)\}, \\ \mathcal{R}(k) &:= \{r_1, r_2, \dots, r_{n(k)}\}, \end{aligned}$$

where $n(k) = \|\mathcal{R}(k)\|$ is the number of the data samples in $\mathcal{D}(k)$. Moreover, the data recorded in the dataset $\mathcal{D}(k)$ can be written in a compact form as:

$$\begin{aligned} X_-(k) &= [\mathbf{x}(r_1), \mathbf{x}(r_2), \dots, \mathbf{x}(r_{n(k)})], \\ U_-(k) &= [\mathbf{u}(r_1), \mathbf{u}(r_2), \dots, \mathbf{u}(r_{n(k)})], \\ W_-(k) &= [\mathbf{w}(r_1), \mathbf{w}(r_2), \dots, \mathbf{w}(r_{n(k)})], \\ X_+(k) &= [\mathbf{x}(r_1+1), \mathbf{x}(r_2+1), \dots, \mathbf{x}(r_{n(k)}+1)]. \end{aligned}$$

In this work, we mainly consider the scenario where the disturbance $\mathbf{w}(k), k \in \mathbb{N}$ is an independent, identically distributed (i.i.d.) stochastic process with zero mean. Note that the assumption of zero mean is commonly adopted in existing literature [48]–[50]; by introducing the bias values of the system state, a nonzero mean disturbance can be further transformed into the equivalent scenario of a zero mean disturbance. Moreover, we assume that the disturbances in matrix $W_-(k)$ satisfy the following property:

$$\mathbb{P}[W_-(k)W_-^T(k) \preceq \Phi_1(n(k), \delta)] \geq \delta, \quad (2)$$

where $\Phi_1(n(k), \delta)$ is a positive semi-definite matrix.

Remark 1. *Inequality (2) is normally called a concentration inequality, which holds for different kinds of disturbances. For the i.i.d. disturbances in matrix $W_-(k)$, the specific parameter $\Phi_1(n(k), \delta)$ is related with the number of the considered data samples $n(k)$ and the probability δ . In practice, the matrix parameter $\Phi_1(n(k), \delta)$ can be obtained according to different kinds of prior knowledge of the disturbance, which allows the application of the proposed results to different scenarios. After completing the design of the ITL mechanism and discussing its related properties, several specific examples for $\Phi_1(\cdot)$ will be briefly discussed in Section III-C.*

To learn the system parameters, we define the admissible set of system parameters (A, B) that can “explain” the dataset $\mathcal{D}(k)$ as

$$\begin{aligned} \Gamma_\delta(\mathcal{D}(k)) \\ := \left\{ (A, B) \mid X_+(k) = AX_-(k) + BU_-(k) + W_-(k) \text{ holds} \right. \\ \left. \text{for some } W_-(k) \text{ satisfying (2)} \right\}. \end{aligned} \quad (3)$$

Let $\mathfrak{V}(\Gamma_\delta(\mathcal{D}(k)))$ be the Lebesgue measure of the set $\Gamma_\delta(\mathcal{D}(k))$. With this notation, the contribution of a new

data sample to reducing the Lebesgue measure of the set-membership estimate $\Gamma_\delta(\mathcal{D}(k))$ can be characterized, which is termed as “innovation” and is introduced in Definition 1.

Definition 1 (ϵ_l -innovative data sample). *For a set $\Gamma_\delta(\mathcal{D}(k))$ defined in (3), a new data sample $(\mathbf{x}(k), \mathbf{u}(k), \mathbf{x}(k+1))$ is called an ϵ_l -innovative data sample if the following inequality hold:*

$$\mathfrak{V}(\Gamma_\delta(\hat{\mathcal{D}}(k+1))) \leq \epsilon_l \mathfrak{V}(\Gamma_\delta(\mathcal{D}(k))), \quad (4)$$

where $\hat{\mathcal{D}}(k+1) := \mathcal{D}(k) \cup \{(\mathbf{x}(k), \mathbf{u}(k), \mathbf{x}(k+1))\}$.

Remark 2. *We note that the concept of “innovation” is borrowed from Kalman filtering [51] and system identification [52] theory. Specifically, similar to its definitions and interpretations in Kalman filters and system identification approaches, the innovativeness of a data sample is defined as the new information contained in it compared to a historical dataset. With this definition, we are able to online evaluate the contribution of an incoming data sample on reducing the Lebesgue measure of the set $\Gamma_\delta(\mathcal{D}(k))$.*

Remark 3. *The ϵ_l -innovation is defined for a particular data sample. The choice of a one-step decision criterion is made mainly based on computational considerations to provide “yes” or “no” answers to an incoming data sample through relatively simple calculations. Evaluating whether a sampled data segment (instead of a data sample) is innovative unavoidably introduces additional computational burden, thereby potentially decreasing the value of introducing the ITL mechanism. We also note that the proposed definition can be easily extended by replacing $(\mathbf{x}(k), \mathbf{u}(k), \mathbf{x}(k+1))$ with data segments.*

With the above descriptions, this work introduces an online data-selection and control-relevant event-triggered learning approach by evaluating the ϵ_l -innovativeness of a data sample. Specifically, the following questions will be investigated:

- How to design a set-membership learning approach such that a set $\Gamma_\delta(\mathcal{D}(k))$ can be constructed?
- How to design an ITL mechanism to balance the learning performance and data efficiency?
- How to design a predictive controller using the model learned from the ITL mechanism?

III. MAIN RESULTS

This section presents the main theoretic developments of the proposed ITL mechanism and its application to data-driven predictive control. We first introduce the proposed ITL approach and provide the corresponding convergence analysis. Then we discuss the parameterization of the concentration inequality (2) for two special cases of disturbances, including bounded deterministic disturbances and stochastic disturbances with known covariance. Finally, we show the applicability of the ITL scheme to data-driven predictive control utilizing a min-max model predictive control approach.

A. Set-membership Learning

In this section, we develop a probabilistic set-membership learning approach compatible with the dataset $\mathcal{D}(k)$ and the concentration inequality (2). To enable the design of the set-membership learning, we parameterize the set $\Gamma_\delta(\mathcal{D}(k))$ as follows:

$$\begin{aligned}\Gamma_\delta(\mathcal{D}(k)) &= \Gamma(\Psi(n(k), \delta), \mathcal{D}(k)) \\ &:= \{(A, B) \mid Z(A, B)\Psi(n(k), \delta)Z^T(A, B) \succeq 0\},\end{aligned}\quad (5)$$

where $Z(A, B) := [I_{n_x} \ A \ B]$ is a function and $\Psi(n(k), \delta)$ is a matrix parameter defined as

$$\Psi(n(k), \delta) := \Xi(k)\tilde{\Psi}(n(k), \delta)\Xi^T(k), \quad (6)$$

$$\Xi(k) := \begin{bmatrix} I_{n_x} & X_+(k) \\ \mathbf{0} & -X_-(k) \\ \mathbf{0} & -U_-(k) \end{bmatrix}, \quad (7)$$

$$\tilde{\Psi}(n(k), \delta) := \begin{bmatrix} \tilde{\Phi}_1(n(k), \delta) & \mathbf{0} \\ \mathbf{0} & -\Phi_2(k) \end{bmatrix}, \quad (8)$$

$$\begin{aligned}\tilde{\Phi}_1(n(k), \delta) &:= \frac{(n_x + n_u)^2}{n(k)} \lambda_1(\Phi_1(n(k), \delta)) I_{n_x}, \\ \Phi_2(k) &:= \begin{bmatrix} X_-(k) \\ U_-(k) \end{bmatrix}^\dagger \begin{bmatrix} X_-(k) \\ U_-(k) \end{bmatrix}.\end{aligned}\quad (9)$$

Using the matrices above, the set-membership estimates of the set of parameters compatible with $\mathcal{D}(k)$ can be obtained as (3). In the next result, we show that the learned parametric uncertainty set $\Gamma(\Psi(n(k), \delta), \mathcal{D}(k))$ contains unknown parameters (A_*, B_*) with a high probability.

Theorem 1. Consider system (1) with an available dataset $\mathcal{D}(k)$. The set $\Gamma(\Psi(n(k), \delta), \mathcal{D}(k))$ defined in (5)-(9) is a convex set and satisfies

$$\mathbb{P}[(A_*, B_*) \in \Gamma(\Psi(n(k), \delta), \mathcal{D}(k))] \geq \delta, \quad (10)$$

if (i) the concentration inequality in (2) is satisfied and (ii) the matrix $[X_-^T(k) \ U_-^T(k)]^T$ has full row rank.

Proof. First, we show that inequality (10) can be proved from (2) and the property of the matrix $W_-(k)\Phi_2(k)W_-^T(k)$. According to the definition of the Moore-Penrose inverse, $\Phi_2(k)$ is a projection matrix, and thus the rank of $\Phi_2(k)$ satisfies

$$\text{rank}(\Phi_2(k)) = n_x + n_u \quad (11)$$

since the matrix $[X_-^T(k) \ U_-^T(k)]^T$ has full row rank. Therefore, the matrix $\Phi_2(k)$ can be diagonalized using a orthogonal matrix $P(k)$ as

$$\Lambda(k) := P(k)\Phi_2(k)P^{-1}(k) = \begin{bmatrix} I_{n_x+n_u} & \mathbf{0} \\ \mathbf{0} & \mathbf{0} \end{bmatrix}, \quad (12)$$

where zero matrices with appropriate dimensions are denoted as $\mathbf{0}$.

Then, we obtain

$$\text{Tr}(W_-(k)\Phi_2(k)W_-^T(k)) \quad (13)$$

$$= \text{Tr}(W_-(k)P^{-1}(k)\Lambda(k)P(k)W_-^T(k))$$

$$= \text{Tr}(\Lambda(k)P(k)W_-^T(k)W_-(k)P^{-1}(k)). \quad (14)$$

Moreover, under the condition that $W_-(k)W_-^T(k) \preceq \Phi_1(n(k), \delta)$, an upper bound for the trace of matrix $W_-(k)\Phi_2(k)W_-^T(k)$ can be obtained using a quantitative form of Sylvester's law of inertia (Theorem 4.5.9 in [53]) as

$$\begin{aligned}&\text{Tr}(W_-(k)\Phi_2(k)W_-^T(k)) \\ &= \text{Tr}(\Lambda(k)P(k)W_-^T(k)W_-(k)P^{-1}(k)) \\ &\leq \frac{(n_x + n_u)^2}{n(k)} \lambda_1(W_-^T(k)W_-(k)).\end{aligned}$$

Furthermore, we note that the nonzero eigenvalues of matrix $W_-(k)W_-^T(k)$ and matrix $W_-^T(k)W_-(k)$ are the same. Thus, from $W_-(k)W_-^T(k) \preceq \Phi_1(n(k), \delta)$, we obtain

$$\begin{aligned}&\frac{(n_x + n_u)^2}{n(k)} \lambda_1(W_-^T(k)W_-(k)) \\ &= \frac{(n_x + n_u)^2}{n(k)} \lambda_1(W_-(k)W_-^T(k)) \\ &\leq \frac{(n_x + n_u)^2}{n(k)} \lambda_1(\Phi_1(n(k), \delta)).\end{aligned}\quad (15)$$

Then, from (14)-(15), the following inequality can be obtained

$$W_-(k)\Phi_2(k)W_-^T(k) \preceq \tilde{\Phi}_1(n(k), \delta). \quad (16)$$

Note that inequality (16) is obtained under the condition that $W_-(k)W_-^T(k) \preceq \Phi_1(n(k), \delta)$, which holds with a probability not less than δ according to (2). Thus, we have

$$\mathbb{P}[\text{Inequality (16) holds}] \geq \delta. \quad (17)$$

By substituting equations (6)-(9) into (17), a property of the unknown parameters (A_*, B_*) can be obtained as

$$\mathbb{P}[Z(A_*, B_*)\Psi(n(k), \delta)Z^T(A_*, B_*) \succeq 0] \geq \delta. \quad (18)$$

According to (3), $\Gamma(\Psi(n(k), \delta), \mathcal{D}(k))$ is defined as a set of all elements (A, B) such that

$$Z(A, B)\Xi(k)\tilde{\Psi}(n(k), \delta)\Xi^T(k)Z^T(A, B) \succeq 0 \quad (19)$$

holds. Therefore, the property of the unknown parameters (18) can be equivalently rewritten as

$$\mathbb{P}[(A_*, B_*) \in \Gamma(\Psi(n(k), \delta), \mathcal{D}(k))] \geq \delta, \quad (20)$$

which completes the proof of (10).

Next, we show that the convexity of the set $\Gamma(\Psi(n(k), \delta), \mathcal{D}(k))$ can be verified according to its definition. Specifically, let $(A_1, B_1), (A_2, B_2) \in \Gamma(\Psi(n(k), \delta), \mathcal{D}(k))$ be two possible parameters. Then, the corresponding disturbance sequences can be defined as

$$W_1 := X_+(k) - A_1 X_-(k) - B_1 U_-(k), \quad (21)$$

$$W_2 := X_+(k) - A_2 X_-(k) - B_2 U_-(k). \quad (22)$$

The set $\Gamma(\Psi(n(k), \delta), \mathcal{D}(k))$ is convex if and only if the following equations hold:

$$Z_\Gamma \Xi(k)\tilde{\Psi}(n(k), \delta)\Xi^T(k)Z_\Gamma^T \succeq 0, \quad (23)$$

$$Z_\Gamma := \theta_\Gamma Z(A_1, B_1) + (1 - \theta_\Gamma)Z(A_2, B_2). \quad (24)$$

where $\theta_\Gamma \in [0, 1]$ is a constant. Moreover, equation (23) can

be equivalently rewritten as

$$\begin{aligned} Z_\Gamma \Xi(k) \tilde{\Psi}(n(k), \delta) \Xi^T(k) Z_\Gamma^T &\succeq 0 \\ \Leftrightarrow W_\Gamma \Phi_2(k) W_\Gamma^T &\preceq \tilde{\Phi}_1(n(k), \delta), \end{aligned} \quad (25)$$

where W_Γ is defined as

$$W_\Gamma := \theta_\Gamma W_1 + (1 - \theta_\Gamma) W_2. \quad (26)$$

Then, using Cauchy-Schwarz inequality, we have

$$\begin{aligned} W_\Gamma \Phi_2(k) W_\Gamma^T &= \theta_\Gamma^2 W_1 \Phi_2(k) W_1^T + (1 - \theta_\Gamma)^2 W_2 \Phi_2(k) W_2^T \\ &\quad + \theta_\Gamma (1 - \theta_\Gamma) (W_1 \Phi_2(k) W_2^T + W_2 \Phi_2(k) W_1^T) \\ &\preceq \theta_\Gamma^2 W_1 \Phi_2(k) W_1^T + (1 - \theta_\Gamma)^2 W_2 \Phi_2(k) W_2^T \\ &\quad + \theta_\Gamma (1 - \theta_\Gamma) (W_1 \Phi_2(k) W_1^T + W_2 \Phi_2(k) W_2^T) \\ &\preceq \tilde{\Phi}_1(n(k), \delta), \end{aligned} \quad (27)$$

which completes the proof. \square

Remark 4. From (10), the performance of the learned parametric uncertainty set $\Gamma(\Psi(n(k), \delta), \mathcal{D}(k))$ can be quantitatively evaluated by the Lebesgue measure ($\mathfrak{V}(\cdot)$) of the set and the confidence level (δ) that indicates the likelihood of true parameters (A_*, B_*) belonging to the set. We note that the confidence level is usually a user-defined requirement related to the performance specifications. In contrast, the size of the uncertainty set is mainly determined by the available data samples. Thus, the innovativeness of a data sample is quantified by its contribution to reducing the Lebesgue measure of the learned uncertainty set while maintaining the pre-specified confidence level.

Write

$$[\hat{A} \ \hat{B}] := X_+(k) \begin{bmatrix} X_-(k) \\ U_-(k) \end{bmatrix}^\dagger. \quad (29)$$

To facilitate our further analysis, the geometric property of the set-membership learning method is analyzed in the next result.

Proposition 1. Consider the set $\Gamma(\Psi(n(k), \delta), \mathcal{D}(k))$ defined in (5)-(9). For $(A, B) \in \Gamma(\Psi(n(k), \delta), \mathcal{D}(k))$, the following claim holds:

$$\begin{aligned} &\left([A \ B] - [\hat{A} \ \hat{B}] \right) \begin{bmatrix} X_-(k) \\ U_-(k) \end{bmatrix} \begin{bmatrix} X_-(k) \\ U_-(k) \end{bmatrix}^\dagger \left([A \ B] - [\hat{A} \ \hat{B}] \right)^T \\ &\preceq \tilde{\Phi}_1(n(k), \delta), \end{aligned} \quad (30)$$

Proof. The set-membership learning method defined in (5)-(9) leads to a set $\Gamma(\Psi(n(k), \delta), \mathcal{D}(k))$ in the form of

$$\begin{aligned} &\Gamma(\Psi(n(k), \delta), \mathcal{D}(k)) \\ &:= \left\{ (A, B) \mid Z(A, B) \Xi(k) \tilde{\Psi}(n(k)) \Xi^T(k) Z^T(A, B) \succeq 0 \right\}. \end{aligned} \quad (31)$$

To prove Proposition 1, we define a matrix $\bar{W}_-(k)$ as

$$\bar{W}_-(k) := X_+(k) - [A \ B] \begin{bmatrix} X_-(k) \\ U_-(k) \end{bmatrix}. \quad (32)$$

By utilizing the defined matrix $\bar{W}_-(k)$, the inequality $Z(A, B) \Xi(k) \tilde{\Psi}(n(k)) \Xi^T(k) Z^T(A, B) \succeq 0$ in (31) can be

equivalently rewritten as

$$\bar{W}_-(k) \Phi_2(k) \bar{W}_-(k)^T \preceq \tilde{\Phi}_1(n(k), \delta). \quad (33)$$

The left side term of inequality (33) can be derived as

$$\begin{aligned} &\bar{W}_-(k) \begin{bmatrix} X_-(k) \\ U_-(k) \end{bmatrix}^\dagger \begin{bmatrix} X_-(k) \\ U_-(k) \end{bmatrix} \bar{W}_-^T(k) \\ &\stackrel{(i)}{=} \bar{W}_-(k) \begin{bmatrix} X_-(k) \\ U_-(k) \end{bmatrix}^\dagger \begin{bmatrix} X_-(k) \\ U_-(k) \end{bmatrix} \begin{bmatrix} X_-(k) \\ U_-(k) \end{bmatrix}^\dagger \begin{bmatrix} X_-(k) \\ U_-(k) \end{bmatrix} \bar{W}_-^T(k) \\ &\stackrel{(ii)}{=} \left(\bar{W}_-(k) \begin{bmatrix} X_-(k) \\ U_-(k) \end{bmatrix}^\dagger \begin{bmatrix} X_-(k) \\ U_-(k) \end{bmatrix} \right) \left(\bar{W}_-(k) \begin{bmatrix} X_-(k) \\ U_-(k) \end{bmatrix}^\dagger \begin{bmatrix} X_-(k) \\ U_-(k) \end{bmatrix} \right)^T, \end{aligned} \quad (34)$$

where the equations in (i)-(ii) are obtained by the definition of Moore-Penrose inverse.

According to (32), we have

$$\begin{aligned} &\bar{W}_-(k) \begin{bmatrix} X_-(k) \\ U_-(k) \end{bmatrix}^\dagger \begin{bmatrix} X_-(k) \\ U_-(k) \end{bmatrix} \\ &= \left(X_+(k) - [A \ B] \begin{bmatrix} X_-(k) \\ U_-(k) \end{bmatrix} \right) \begin{bmatrix} X_-(k) \\ U_-(k) \end{bmatrix}^\dagger \begin{bmatrix} X_-(k) \\ U_-(k) \end{bmatrix}. \end{aligned} \quad (35)$$

Since the matrix $[X_-^T(k) \ U_-^T(k)]^T$ has full row rank, the equation (35) can be further reformulated as

$$\begin{aligned} &\bar{W}_-(k) \begin{bmatrix} X_-(k) \\ U_-(k) \end{bmatrix}^\dagger \begin{bmatrix} X_-(k) \\ U_-(k) \end{bmatrix} \\ &= \left(X_+(k) \begin{bmatrix} X_-(k) \\ U_-(k) \end{bmatrix}^\dagger - [A \ B] \right) \begin{bmatrix} X_-(k) \\ U_-(k) \end{bmatrix}. \end{aligned} \quad (36)$$

By substituting (36) in (34) (namely, the left side term of inequality (33)), the proof of proposition 1 is completed. \square

Remark 5. Proposition 1 reveals the relationship between the proposed set-membership learning method defined in (5)-(9) and the point-valued estimate (29). The estimate defined in (29) is generally known as the least squares estimation of unknown parameters (A_*, B_*) . According to Proposition 1, the set obtained in (10) is a convex set centered at the least squares estimate, and it is also influenced by the utilized data samples $[X_-^T(k) \ U_-^T(k)]^T$ and the parameter $\tilde{\Phi}_1(n(k), \delta)$.

B. Innovation-triggered Learning

In this section, we focus on the online update of the data index set $\mathcal{R}(k)$, and introduce the proposed innovation-triggered learning approach. From Proposition 1, we observe that the form of the set $\Gamma(\Psi(n(k), \delta), \mathcal{D}(k))$ is similar to an ellipsoid, the Lebesgue measure of which can be easily calculated according to [54, Section 2.1]. Based on this observation, an ITL can be designed.

Define

$$T(k) := \left(\begin{bmatrix} X_-(k) \\ U_-(k) \end{bmatrix} \begin{bmatrix} X_-(k) \\ U_-(k) \end{bmatrix}^T \right)^{-1}. \quad (37)$$

Then the ITL mechanism can be described by the update of

the index set $\mathcal{R}(k)$ as

$$\mathcal{R}(k) = \begin{cases} \mathcal{R}(k-1), & \text{if (39) holds,} \\ \mathcal{R}(k-1) \cup \{k-1\}, & \text{otherwise,} \end{cases} \quad (38)$$

$$\frac{|\tilde{T}(k-1)|}{|T(k-1)|} \geq \epsilon_l^2 \left(\frac{\text{Tr}[\tilde{\Phi}_1(n(k-1), \delta)]}{\text{Tr}[\tilde{\Phi}_1(n(k-1)+1, \delta)]} \right)^{n_x(n_x+n_u)}, \quad (39)$$

where $\epsilon_l \in (0, 1)$ is a constant, and $\tilde{T}(k)$ is

$$\tilde{T}(k) = \left(\begin{bmatrix} X_-(k) \\ U_-(k) \end{bmatrix} \begin{bmatrix} X_-(k) \\ U_-(k) \end{bmatrix}^T + \begin{bmatrix} \mathbf{x}(k) \\ \mathbf{u}(k) \end{bmatrix} \begin{bmatrix} \mathbf{x}(k) \\ \mathbf{u}(k) \end{bmatrix}^T \right)^{-1}. \quad (40)$$

In (38), an updating mechanism is proposed for the index set $\mathcal{R}(k)$, based on which the data set $\mathcal{D}(k)$ and the learned stochastic parametric uncertainty set $\Gamma(\Psi(n(k), \delta), \mathcal{D}(k))$ can be updated accordingly. For the ITL mechanism, the asymptotic property of the set $\Gamma(\Psi(n(k), \delta), \mathcal{D}(k))$ is further analyzed in the following result.

Theorem 2. Consider the system in (1) and the disturbance $\mathbf{w}(k)$ satisfying (2). If the dataset $\mathcal{D}(k)$ is updated according to the ITL mechanism (38), the Lebesgue measure of the set $\Gamma(\Psi(n(k), \delta), \mathcal{D}(k))$ defined in (5)-(9) converges exponentially with the increase of $n(k)$ such that

$$\mathfrak{V}(\Gamma(\Psi(n(k), \delta), \mathcal{D}(k))) \leq \epsilon_l^{n(k)} \mathfrak{V}_0, \quad k > k_0 \quad (41)$$

holds for some $\mathfrak{V}_0 > 0$ and

$$k_0 = \inf \{k \mid \text{rank}([X_-^T(k) \ U_-^T(k)]^T) = n_x + n_u\}.$$

Proof. To prove this theorem, we first note that the inequality in (16) leads to

$$\tilde{\Phi}_1(n(k), \delta) - \bar{W}_-(k) \Phi_2(k) \bar{W}_-(k)^T \succeq 0 \quad (42)$$

$$\Rightarrow \text{Tr}[\tilde{\Phi}_1(n(k), \delta) - \bar{W}_-(k) \Phi_2(k) \bar{W}_-(k)^T] \geq 0. \quad (43)$$

To calculate the Lebesgue measure of the set $\Gamma(\Psi(n(k), \delta), \mathcal{D}(k))$, we introduce the vectorization function $\text{Vec}([A \ B]) : \mathbb{R}^{n_x \times (n_x+n_u)} \rightarrow \mathbb{R}^{(n_x^2+n_xn_u) \times 1}$. From (5)-(9) and the inequality in (43), we have

$$\begin{aligned} & \text{Vec}([A \ B] - [\hat{A} \ \hat{B}]) \left(\begin{bmatrix} X_-(k) \\ U_-(k) \end{bmatrix} \begin{bmatrix} X_-(k) \\ U_-(k) \end{bmatrix}^T \otimes I_{n_x} \right) \\ & \quad \cdot \text{Vec}([A \ B] - [\hat{A} \ \hat{B}])^T \\ & \leq \text{Tr} \left[\frac{(n_x+n_u)^2}{n(k)} \lambda_1(\Phi_1(n(k), \delta)) I_{n_x} \right] \\ & \leq \frac{n_x(n_x+n_u)^2}{n(k)} \lambda_1(\Phi_1(n(k), \delta)). \end{aligned} \quad (45)$$

By defining $\tilde{\Gamma}(\Psi(n(k), \delta), \mathcal{D}(k))$ as

$$\tilde{\Gamma}(\Psi(n(k), \delta), \mathcal{D}(k)) := \left\{ [A \ B] \mid \text{Inequality (45) holds} \right\}, \quad (46)$$

(43) leads to the inclusion relation as

$$\Gamma(\Psi(n(k), \delta), \mathcal{D}(k)) \subseteq \tilde{\Gamma}(\Psi(n(k), \delta), \mathcal{D}(k)). \quad (47)$$

From (45), the mapped set $\text{Vec}(\tilde{\Gamma}(\Psi(n(k), \delta), \mathcal{D}(k)))$ is an ellipsoid in $\mathbb{R}^{(n_x^2+n_xn_u) \times 1}$. Thus we claim that the image of set $\Gamma(\Psi(n(k), \delta), \mathcal{D}(k))$ in $\mathbb{R}^{(n_x^2+n_xn_u) \times 1}$ is enveloped by the ellipsoid defined in (45).

According to [54, Section 2.1], the volume of the ellipsoid $\text{Vec}(\tilde{\Gamma}(\Psi(n(k), \delta), \mathcal{D}(k)))$ can be calculated as

$$\begin{aligned} & \mathfrak{V} \left(\text{Vec} \left(\tilde{\Gamma}(\Psi(n(k), \delta), \mathcal{D}(k)) \right) \right) \\ & = \left(\text{Tr}[\tilde{\Phi}_1(n(k), \delta)] \right)^{\frac{n_x(n_x+n_u)}{2}} |T(k)|^{\frac{1}{2}}. \end{aligned} \quad (48)$$

Now we are ready to analyze the convergence of the ITL mechanism designed in (38)-(40). In the case that $\mathcal{R}(k) = \mathcal{R}(k-1)$, the number $n(k)$, the dataset $\mathcal{D}(k)$, and the size $\mathfrak{V}(\Gamma(\Psi(n(k), \delta), \mathcal{D}(k)))$ do not change compared to the time instant $k-1$. Thus the following analysis concentrates on the case that $\mathcal{R}(k) = \mathcal{R}(k-1) \cup \{k-1\}$.

In the case $\mathcal{R}(k) = \mathcal{R}(k-1) \cup \{k\}$, the following inequality can be obtained according to (39):

$$\frac{|\tilde{T}(k-1)|^{\frac{1}{2}}}{|T(k-1)|^{\frac{1}{2}}} < \epsilon_l \left(\frac{\text{Tr}[\tilde{\Phi}_1(n(k-1), \delta)]}{\text{Tr}[\tilde{\Phi}_1(n(k-1)+1, \delta)]} \right)^{\frac{n_x(n_x+n_u)}{2}}. \quad (49)$$

Then the measure $\mathfrak{V}(\tilde{\Gamma}(\Psi(n(k), \delta), \mathcal{D}(k)))$ satisfies

$$\begin{aligned} & \mathfrak{V}(\tilde{\Gamma}(\Psi(n(k), \delta), \mathcal{D}(k))) \\ & \leq \epsilon_l \mathfrak{V}(\tilde{\Gamma}(\Psi(n(k-1), \delta), \mathcal{D}(k-1))). \end{aligned} \quad (50)$$

Then, by writing

$$\mathfrak{V}_0 = \mathfrak{V}(\tilde{\Gamma}(\Psi(n(k_0), \delta), \mathcal{D}(k_0))),$$

the proof of the claim in (41) is completed. \square

Remark 6. In the proof Theorem 2, the relationship between the set $\Gamma(\Psi(n(k), \delta), \mathcal{D}(k))$ defined in (5)-(9) and an ellipsoid is characterized in (45). The relationship facilitates the convergence analysis of the ITL mechanism in (38) by converting the calculation of the measure of a matrix ellipsoid to the calculation of the volume of a vector ellipsoid, which is easier to calculate and analyze with the tools of ellipsoidal analysis [54]. Specifically, the image of the set $\Gamma(\Psi(n(k), \delta), \mathcal{D}(k))$ in space $\mathbb{R}^{(n_x^2+n_xn_u) \times 1}$ is contained in an ellipsoid $\text{Vec}(\tilde{\Gamma}(\Psi(n(k), \delta), \mathcal{D}(k)))$. The convergence property of the learned set $\Gamma(\Psi(n(k), \delta), \mathcal{D}(k))$ can thus indirectly obtained by analyzing the ellipsoid.

Next, we briefly show how to find a stabilizing controller with the proposed ITL. Before continuing, we first recall the definition of informativity-based stabilizing controller (ISC) (which is a generalized version of Definition 3 in [12]).

Definition 2 (ISC). Let $\mathcal{D}(k)$ be a set of data samples of system (1), and $\Gamma(\Psi(n(k), \delta), \mathcal{D}(k))$ be a set of unknown system parameters defined as (3). Then, a controller $\mathfrak{C}(\mathbf{x}) : \mathbb{R}^{n_x} \rightarrow \mathbb{R}^{n_u}$ is called an ISC if the controller $\mathbf{u} = \mathfrak{C}(\mathbf{x})$ stabilizes all systems in the set $\Gamma(\Psi(n(k), \delta), \mathcal{D}(k))$.

Using the above definition, a sufficient condition for the

existence of an ISC is shown in Proposition 2.

Proposition 2. *An ISC $K(k)$ can be obtained using dataset $\mathcal{D}(k)$ if there exist matrices $P \in \mathbb{R}^{n_x \times n_x}$, $P = P^T \succ 0$, $L \in \mathbb{R}^{n_u \times n_x}$, and scalars $\xi \geq 0$, $\rho > 0$ satisfying*

$$\begin{bmatrix} P - \rho I_{n_x} & \mathbf{0} & \mathbf{0} & \mathbf{0} \\ \mathbf{0} & -P & -L^T & \mathbf{0} \\ \mathbf{0} & -L & \mathbf{0} & L \\ \mathbf{0} & \mathbf{0} & L^T & P \end{bmatrix} - \xi \check{\Xi}(k) \Psi(n(k)) \check{\Xi}^T(k) \succeq 0, \quad (51)$$

where

$$\check{\Xi}(k) := \begin{bmatrix} \Xi(k) \\ \mathbf{0}_{n_x \times (n(k)+n_x)} \end{bmatrix}.$$

Moreover, if P and L satisfy (51), then $K(k) := LP^{-1}$ is a stabilizing feedback gain for $(A, B) \in \Gamma(\Psi(n(k), \delta), \mathcal{D}(k))$.

Proof. This result can be proved following a similar line of arguments to the proof of Theorem 14 in [12] with the help of the matrix S-lemma [55], and thus the proof is omitted. \square

C. Discussions on Special Concentration Inequalities

Different parameterizations of the concentration inequality in (2) can be obtained if different prior knowledge of the disturbance is available. In this subsection, we discuss two important examples, including deterministic disturbances with known upper bounds and stochastic disturbances with known covariance; additional examples can refer to [56].

Case I: Deterministic disturbances with known upper bounds. For bounded disturbance $\mathbf{w}(k) \mathbf{w}^T(k) \preceq \bar{\phi}$ with parameters set as

$$\delta = 1, \quad \Phi_1(n(k), \delta) = n(k) \bar{\phi}, \quad (52)$$

an equation in the form of (2) can be obtained as

$$\mathbb{P}[W_-(k) W_-^T(k) \preceq n(k) \bar{\phi}] = 1. \quad (53)$$

This case is practical since disturbance signals in engineering applications are usually bounded. A conservative upper bound $\bar{\phi}$ suffices to obtain the parameter $\Phi_1(n(k), \delta)$ in (2).

Case II: Stochastic disturbances with covariance information. Let σ_w be the covariance matrix of the stochastic disturbance $\mathbf{w}(k)$. Then for the random matrix

$$W_-(k) W_-^T(k) = \sum_{i \in \mathcal{R}(k)} \mathbf{w}(i) \mathbf{w}^T(i) \succeq 0,$$

the expectation of which can be denoted as

$$\mathbb{E}[W_-(k) W_-^T(k)] = n(k) \sigma_w.$$

Before discussing the parameterization of the concentration inequality for this case, we introduce an instrumental lemma as follows.

Lemma 1 (Theorem 12 in [57]). *Let $\Phi \succ 0$ be a matrix parameter, and let X be a random matrix such that $X \succ 0$ almost surely. Then the following inequality holds:*

$$\mathbb{P}[X \not\preceq \Phi] \leq \text{Tr}(\mathbb{E}[X] \Phi^{-1}). \quad (54)$$

According to Lemma 1, an inequality can be obtained as

$$\begin{aligned} & \mathbb{P}(\Phi(n(k)) - W_-(k) W_-^T(k) \succeq 0) \\ & \geq 1 - \text{Tr}(\mathbb{E}[W_-(k) W_-^T(k)] \Phi^{-1}(n(k))), \end{aligned} \quad (55)$$

and a concentration inequality for Case II can be further obtained in the following lemma.

Lemma 2. *For $\delta \in (0, 1)$ and a random variable $\mathbf{w}(k)$ with covariance matrix σ_w , equation (2) holds if*

$$\Phi_1(n(k), \delta) = \frac{n_x n(k)}{1 - \delta} \sigma_w. \quad (56)$$

Proof. According to the definition of covariance matrix, the item $W_-(k) W_-^T(k)$ can be seen as a random matrix with an expectation being $\mathbb{E}[W_-(k) W_-^T(k)] = n(k) \sigma_w$. For the parameter $\Phi_1(n(k), \delta)$ provided in (56), the following equations hold:

$$\begin{aligned} & \mathbb{P}(\Phi_1(n(k), \delta) - W_-(k) W_-^T(k) \succeq 0) \\ & = \mathbb{P}(W_-(k) W_-^T(k) \preceq \Phi_1(n(k), \delta)) \\ & \geq 1 - \text{Tr}(\mathbb{E}[W_-(k) W_-^T(k)] \Phi_1^{-1}(n(k), \delta)) = \delta, \end{aligned} \quad (57)$$

which completes the proof. \square

Remark 7. *In engineering applications, the covariance of the disturbance can be estimated from data samples even if the system parameters are unknown. For instance, [58] provided a model-free estimation approach for the disturbance variance. On the other hand, although an accurate estimate of the covariance σ_w may be unavailable in practice, it can be replaced by its upper bound $\bar{\sigma}_w$ and Lemma 2 still holds. Using an upper bound of the covariance $\bar{\sigma}_w$, the parameter $\Phi_1(n(k), \delta)$ can be selected as $\frac{n_x n(k)}{1 - \delta} \bar{\sigma}_w$ to ensure inequality (2), which can be proved similarly to Lemma 2.*

D. Applications to Data-driven Predictive Control

In this section, we show how the proposed ITL mechanism can be utilized in data-drive predictive control. Compared with standard predictive controllers, the proposed mechanisms lead to intermittent updates of $\mathcal{D}(k)$, $K(k)$, and $\Gamma(\Psi(n(k), \delta), \mathcal{D}(k))$, which adds challenges to closed-loop performance analysis. To address this issue, this section focuses on how the uncertainties induced by the ITL can be suitably dealt with to ensure the closed-loop stability of the predictive controller.

Similar to [59]–[62], we parameterize the controller as

$$\mu_c(\mathbf{x}(k), \mathbf{v}(k)) := \mathbf{v}(k) + K(k) \mathbf{x}(k). \quad (58)$$

Here, the feedback gain $K(k)$ is obtained from (51), and $\mathbf{v}(k)$ is the decision variable in predictive controller.

The stage cost function is defined as

$$l(\mathbf{x}, \mathbf{u}) := \mathbf{x}^T Q \mathbf{x} + \mathbf{u}^T R \mathbf{u},$$

where Q and R are positive definite and symmetric matrices. Let $\delta_M > 0$ be a positive constant, then the terminal cost

function is designed as

$$\begin{aligned} V_f(\mathbf{x}; P_f(k)) &:= \mathbf{x}^T P_f(k) \mathbf{x}, \\ P_f(k) &= Q + K^T(k) R K(k) + \delta_M I. \end{aligned} \quad (59)$$

Let \mathbb{W}_{δ_1} be a compact set satisfying

$$\mathbb{P}(\mathbf{w} \in \mathbb{W}_{\delta_1}) \geq \delta_1. \quad (60)$$

For different kinds of disturbances, the set \mathbb{W}_{δ_1} can be obtained using (2).

Let L_f be a local Lipschitz constant of the terminal cost function $V_f(\cdot)$ with the domain being a compact set \mathbb{W}_{δ_1} that contains the origin. For a compact set \mathbb{X} , the parameter θ_f can be designed as

$$\begin{aligned} \theta_f &= \arg \min_{\theta} \theta \\ \text{s.t. } \theta &\geq \mathbf{x}^T \delta_M \mathbf{x} + L_f \max_{\mathbf{w} \in \mathbb{W}_{\delta_1}} \|\mathbf{w}\|, \quad \mathbf{x} \in \mathbb{X}. \end{aligned} \quad (61)$$

For θ_f designed as (61), the terminal constraint set is defined as $\mathbb{X}_f(k) := \{\mathbf{x} | \mathbf{x}^T P_f(k) \mathbf{x} \leq \theta_f\}$.

Let N be the length of the prediction horizon, and write a series of control inputs as

$$\begin{aligned} \boldsymbol{\mu}_c(k; N) &:= \{\mu_c(\mathbf{x}(k), \mathbf{v}(k)), \mu_c(\bar{\mathbf{x}}(k+1), \mathbf{v}(k+1)), \\ &\dots, \mu_c(\bar{\mathbf{x}}(k+N), \mathbf{v}(k+N))\}, \end{aligned}$$

where $\bar{\mathbf{x}}(k+i)$, $i \in \{1, 2, \dots, N\}$ is the predicted state defined as

$$\bar{\mathbf{x}}(k+i) := \Phi_p(i; \mathbf{x}(k), \boldsymbol{\mu}_c(k; N), \hat{\mathbf{W}}(k; N)).$$

Here, $\Phi_p(i; (\mathbf{x}(k), \boldsymbol{\mu}_c(k; N), \hat{\mathbf{W}}(k; N)))$ is the solution of the prediction model with A, B as

$$\begin{aligned} \bar{\mathbf{x}}(k+i+1) &= A\bar{\mathbf{x}}(k+i) + B\mu_c(\bar{\mathbf{x}}(k+i), \mathbf{v}(k+i)) + \hat{\mathbf{w}}(k+i), \end{aligned} \quad (62)$$

where the initial state is $\bar{\mathbf{x}}(k) = \mathbf{x}(k)$, $\hat{\mathbf{w}}(k+i) \in \mathbb{W}_{\delta_1}$, $i \in \{0, 1, \dots, N-1\}$, and $\hat{\mathbf{W}}(k; N)$ is a series of disturbances as

$$\hat{\mathbf{W}}(k; N) := \{\hat{\mathbf{w}}(k), \hat{\mathbf{w}}(k+1), \dots, \hat{\mathbf{w}}(k+N-1)\}. \quad (63)$$

The disturbances used in the prediction model (62) are marked by “ $\hat{\cdot}$ ” to distinguish it from the unknown disturbance in system (1).

Utilizing the variables defined above, the cost function can be defined as

$$\begin{aligned} J_N(\mathbf{x}(k), \boldsymbol{\mu}_c(k; N), \hat{\mathbf{W}}(k; N); A, B) & \quad (64) \\ &:= \sum_{i=0}^{N-1} l(\bar{\mathbf{x}}(k+i), \mu_c(\bar{\mathbf{x}}(k+i), \mathbf{v}(k+i))) + V_f(\bar{\mathbf{x}}(N)). \end{aligned}$$

We note that the aim of the predictive control is to minimize the cost function (64) by choosing appropriate parameters of the controller $\mathbf{v}(k), \mathbf{v}(k+1), \dots, \mathbf{v}(k+N-1)$ using a min-max optimization framework, since the adopted framework can deal with parametric uncertainties. The worst-case cost function is

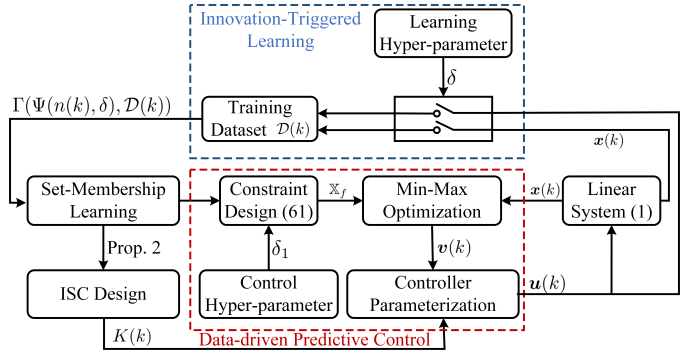


Fig. 1: Schematic diagram of proposed innovation-triggered learning and data-driven predictive control schemes.

written as

$$\begin{aligned} & V_N(\mathbf{x}(k); \boldsymbol{\mu}_c(k; N)) \\ &:= \max_{\hat{\mathbf{W}}(k; N), A, B} J_N(\mathbf{x}(k), \boldsymbol{\mu}_c(k; N), \hat{\mathbf{W}}(k; N); A, B) \\ \text{s.t. } & \hat{\mathbf{W}}(k; N) \in \mathbb{W}_{\delta_1}^N, \quad \bar{\mathbf{x}}(k) = \mathbf{x}(k), \\ & (A, B) \in \Gamma(\Psi(n(k), \delta), \mathcal{D}(k)), \\ & \bar{\mathbf{x}}(k+i) = A\bar{\mathbf{x}}(k+i-1) + B\mu_c(\bar{\mathbf{x}}(k+i-1), 0) \\ & \quad + \hat{\mathbf{w}}(k+i-1), \\ & \mu_c(\bar{\mathbf{x}}(k+i-1), 0) = K(k)\bar{\mathbf{x}}(k+i-1), \quad i \in \{1, \dots, N\}. \end{aligned} \quad (65)$$

Write $\hat{\mathbf{W}}^*(k; N)$ as the worst-case disturbance in the optimization problem (65),

$$\hat{\mathbf{W}}^*(k; N) := \{\hat{\mathbf{w}}^*(k), \hat{\mathbf{w}}^*(k+1), \dots, \hat{\mathbf{w}}^*(k+N-1)\}, \quad (66)$$

Similarly, the worst-case parameters that maximize (65) are denoted as A^*, B^* .

To minimize the cost function at the worst-case condition, the data-driven predictive controller designed in this work is described as

$$\begin{aligned} & \min_{\mathbf{v}(k), \dots, \mathbf{v}(k+N-1)} V_N(\mathbf{x}(k); \boldsymbol{\mu}_c(k; N)) \\ \text{s.t. } & \bar{\mathbf{x}}(k) = \mathbf{x}(k) \\ & \bar{\mathbf{x}}(k+i+1) = A^* \bar{\mathbf{x}}(k+i) + B^* \mu_c(\bar{\mathbf{x}}(k+i), \mathbf{v}(k+i)) \\ & \quad + \hat{\mathbf{w}}^*(k+i), \quad i \in \{0, \dots, N-1\}, \\ & \bar{\mathbf{x}}(k+i) \in \mathbb{X}, \quad i \in \{0, \dots, N\}, \\ & \bar{\mathbf{x}}(k+N) \in \mathbb{X}_f(k), \quad \mu_c(\bar{\mathbf{x}}(k+N), \mathbf{v}(k+N)) \in \mathbb{U}. \end{aligned} \quad (67)$$

In the optimization problem (67), \mathbb{X} and \mathbb{U} are the state and input constraints, respectively. The constraints are determined by operation limits, physical restrictions, cost requirements in practice, etc. For the parameter θ_f obtained as (61), it is assumed that $\mathbb{X}_f \in \mathbb{X}$. Write the optimal cost function as $V_N^*(\mathbf{x}(k))$ and the optimal sequence for $\mathbf{v}(k+i)$ as $\mathbf{v}^*(k+i)$, $i \in \{0, \dots, N-1\}$. Then the optimal control sequence obtained at the time instant k is denoted as $\boldsymbol{\mu}_c^*(k; N)$. The innovation-triggered learning and data-driven predictive control schemes are shown in Fig. 1.

The proposed data-driven predictive control approach is summarized in Algorithm 1.

For the proposed ITL-based predictive controller and the

Algorithm 1 Innovation-triggered learning and data-driven predictive control algorithm.

- 1: Parameters initialization, including δ , δ_1 , Q , R , δ_M , N , σ_w (or $\bar{\phi}$);
- 2: Starting process: test the system dynamics with the designed open-loop control signal until an ISC, $K(\bar{k}_0)$, can be obtained according to (51);
- 3: Calculate a set \mathbb{W}_{δ_1} that satisfies (60);
- 4: **for** $k \geq \bar{k}_0$ **do**
- 5: Update dataset $\mathcal{D}(k)$ according to the innovation-triggered learning mechanism (38);
- 6: **if** $k \in \mathcal{R}(k)$ **then**
- 7: Update $K(k)$ according to (51);
- 8: Update the uncertainty set $\Gamma(\Psi(n(k), \delta), \mathcal{D}(k))$ as (5)-(9);
- 9: **end if**
- 10: Calculate the worst case disturbance sequence $\hat{W}^*(k; N)$ and parameters A^*, B^* by solving the maximum optimization problem (65);
- 11: Calculate the optimal control sequence by solving the minimum optimization problem (67);
- 12: **end for**

parameters designed in (59)-(61), we show that the following results hold, which will be used in the stability analysis of the controller.

Lemma 3. Consider the system in (1) with dataset $\mathcal{D}(k)$ obtained according to the ITL mechanism (38) and the terminal cost function $V_f(\cdot; P_f(k))$ obtained as (59). The inequality

$$\begin{aligned} & V_f(A\mathbf{x}(k) + BK(k)\mathbf{x}(k); P_f(k+1)) \\ & \leq V_f(\mathbf{x}(k); P_f(k)) - l(\mathbf{x}(k), \mathbf{u}(k)) \end{aligned} \quad (68)$$

holds for $\mathbf{x} \in \mathbb{X}$, $(A, B) \in \Gamma(\Psi(n(k), \delta), \mathcal{D}(k))$ if there exists $\xi > 0$ such that

$$\begin{bmatrix} P_f^{-1}(k+1) & \mathbf{0} \\ \mathbf{0} & -\begin{bmatrix} I \\ K(k) \end{bmatrix} \frac{1}{\delta_M} I [I \ K^T(k)] \\ & -\xi \Xi(k) \tilde{\Psi}(n(k)) \Xi^T(k) \end{bmatrix} \succeq 0 \quad (69)$$

holds for $\delta_M > 0$ with the matrix $K(\cdot)$ obtained according to the LMI (51).

Proof. For $(A, B) \in \Gamma(\Psi(n(k), \delta), \mathcal{D}(k))$, the following inequality is satisfied according to (3)

$$Z(A, B)\Xi(k)\tilde{\Psi}(n(k))\Xi^T(k)Z^T(A, B) \succeq 0. \quad (70)$$

Thus, the following inequality can be obtained from (69) and matrix S-lemma [55]:

$$P_f^{-1}(k+1) - [A + BK(k)] \frac{I}{\delta_M} [A + BK(k)]^T \succeq 0. \quad (71)$$

In view of that matrix $P_f(k)$ is a symmetric and positive definite matrix according to (59), we denote

$$P_f(k) = S(k)\Lambda_f(k)S^{-1}(k), \quad (72)$$

$$P_f^{-1}(k) = S(k)\Lambda_f^{-1}(k)S^{-1}(k), \quad (73)$$

where $S(k)$ is invertible matrix and $\Lambda_f(k)$ is a diagonal matrix. By left and right multiplying $P_f(k)$ to matrix

$$P_f(k) := P_f^{-1}(k) - P_f^{-1}(k)[Q + K^T(k)R(k)K(k)]P_f^{-1}(k),$$

the following identity can be obtained

$$\begin{aligned} & P_f(k)P_l(k)P_f(k) \\ & = P_f(k) - [Q + K^T(k)R(k)K(k)] = \delta_M I. \end{aligned} \quad (74)$$

Then matrix $P_l(k)$ can be equivalently written as

$$P_l(k) = S(k)\delta_M\Lambda_f^{-2}(k)S^{-1}(k), \quad (75)$$

based on which we have

$$\frac{I}{\delta_M} = P_f^{-1}(k)P_l^{-1}(k)P_f^{-1}(k). \quad (76)$$

With (76), Inequality (71) leads to

$$\begin{aligned} & P_f^{-1}(k+1) \\ & \succeq [(A + BK(k))P_f^{-1}(k)]P_l^{-1}(k)[(A + BK(k))P_f^{-1}(k)]^T. \end{aligned} \quad (77)$$

Then, by noting that $P_l(k)$ is a positive definite matrix, the following inequality can be obtained according to Schur complement argument,

$$\begin{bmatrix} P_l(k) & [(A + BK(k))P_f^{-1}(k)]^T \\ [(A + BK(k))P_f^{-1}(k)] & P_f^{-1}(k+1) \end{bmatrix} \succeq 0,$$

which further leads to

$$\begin{aligned} & P_l(k) \\ & = P_f^{-1}(k) - P_f^{-1}(k)[Q + K^T(k)R(k)K(k)]P_f^{-1}(k) \\ & \succeq [(A + BK(k))P_f^{-1}(k)]^T P_f(k+1) [(A + BK(k))P_f^{-1}(k)]. \end{aligned} \quad (78)$$

As a result, the proof of claim (68) is completed by left and right multiplying $P_f(k)$ to (78). \square

Note that the condition in (69) is a data-based LMI with the only unknown parameter being the scalar ξ , which can be easily tested. In addition, this condition only needs to be evaluated during an event instant when a new data sample is incorporated into $\mathcal{D}(k)$, since the parameters remain constant during a non-event instant.

Lemma 4. For $\mathbf{x} \in \mathbb{X}_f(k)$ and θ_f designed as (61), there exists $\mathbf{u} = K(k)\mathbf{x}(k)$ such that

$$\bar{A}\mathbf{x} + \bar{B}\mathbf{u} + \mathbf{w} \in \mathbb{X}_f(k+1) \quad (79)$$

holds if (68) is satisfied for $\mathbf{w} \in \mathbb{W}_{\delta_1}$.

Proof. This lemma can be directly verified by noting (61) and thus the proof is omitted. \square

For a feedback control gain $K(k)$ such that inequalities (68) and (79) hold, we define δ_2 as

$$\delta_2 := \max_{\mathbf{w}, \bar{A}, \bar{B}} V_f(\bar{A}\mathbf{x} + \bar{B}\mathbf{u} + \mathbf{w}; P_f(k+1)) \quad (80)$$

$$- V_f(\mathbf{x}; P_f(k)) + l(\mathbf{x}, K(k)\mathbf{x})$$

$$\text{s.t. } \mathbf{w} \in \mathbb{W}_{\delta_1}, \quad \mathbf{x} \in \mathbb{X}, \quad (\bar{A}, \bar{B}) \in \Gamma(\Psi(n(k), \delta), \mathcal{D}(k)).$$

In this work, the cost function (64) is designed as a quadratic

and positive definite function, thus we have

$$l(\mathbf{x}, \mathbf{u}) \geq c_1 |\mathbf{x}|^2, \quad V_N^*(\mathbf{x}) \leq c_2 |\mathbf{x}|^2, \quad \forall \mathbf{x} \in \mathbb{X},$$

with $c_1, c_2 > 0$ being positive constants. Now we are ready to analyze the stability of the closed-loop system by applying the designed data-driven predictive controller with the proposed innovation-triggered learning mechanism.

Proposition 3. Let $\gamma := 1 - \frac{c_1}{c_2}, c := \frac{\delta_2 + \epsilon}{1 - \gamma}$ with δ_2 defined in (80) and $\epsilon > 0$. For system (1) with the dataset obtained by the proposed innovation-triggered learning mechanisms such that (69) holds, the data-driven predictive controller (67) satisfies:

(1) the set $\text{lev}_c(V_N^*) := \{\mathbf{x} | V_N^*(\mathbf{x}) \leq c\}$ is a positive invariant set with probability $\delta\delta_1$, i.e., for $\mathbf{x} \in \text{lev}_c(V_N^*)$, we have

$$\mathbb{P}(A_*\mathbf{x} + B_*\mu_c^*(\mathbf{x}, \mathbf{v}^*) + \mathbf{w} \in \text{lev}_c(V_N^*)) \geq \delta\delta_1; \quad (81)$$

(2) if $\mathbf{x} \in \mathbb{X}, V_N^*(\mathbf{x}) > c$, the state is steered closer to the positive invariant set $\text{lev}_c(V_N^*)$ with a step larger than ϵ with probability $\delta\delta_1$, i.e., for $d := V_N^*(\mathbf{x}) > c$:

$$\mathbb{P}(V_N^*(A_*\mathbf{x} + B_*\mu_c^*(\mathbf{x}, \mathbf{v}^*) + \mathbf{w}) \leq d - \epsilon) \geq \delta\delta_1. \quad (82)$$

Proof. Given that (69) holds, inequalities (68) and (79) can be obtained according to Lemmas 3-4, respectively. Then, the proof of this proposition can be performed by taking $V_N^*(\mathbf{x}(k))$ as a Lyapunov function following a similar line of arguments to Section 3.4 in [63]. \square

IV. NUMERICAL EXAMPLES

In this section, numerical results are shown to verify the proposed results and to compare with other methods. In what follows, the results in Theorems 1-2 are first validated through extensive numerical simulations. Then, comparative simulations are performed to compare the performance of the proposed ITL-based data-driven predictive control approach with DeePC [27] and robust reinforcement learning (RRL) [10]. Finally, the effect of the hyper-parameter is analyzed by considering different choices of δ .

In the simulations, the proposed innovation-triggered learning approach and the data-driven controller are implemented as follows. First, after initializing the performance parameters δ_1, δ , the set \mathbb{W}_{δ_1} is obtained according to (60) and the high-probability region $\Gamma(\Psi(n(k), \delta), \mathcal{D}(k))$ is calculated using dataset $\mathcal{D}(k)$ according to (5). Second, a feedback control gain $K(k)$ is obtained from Proposition 2 after the obtained dataset satisfies the ISC condition (51). Third, using the parameterization approach (58), the data-driven predictive controller is designed as (67).

A. Verification of Theorems 1 and 2

In this subsection, 9,000 third-order linear systems are generated randomly with $\lambda_i(A) \in [-3, 3], i \in \{1, 2, 3\}$. For each linear system, a trajectory is generated with random initial states and inputs. Using the collected data samples in the trajectory, an uncertainty set $\Gamma(\Psi(n(k), \delta), \mathcal{D}(k))$ is learned for the system parameters according to Theorem 1. We

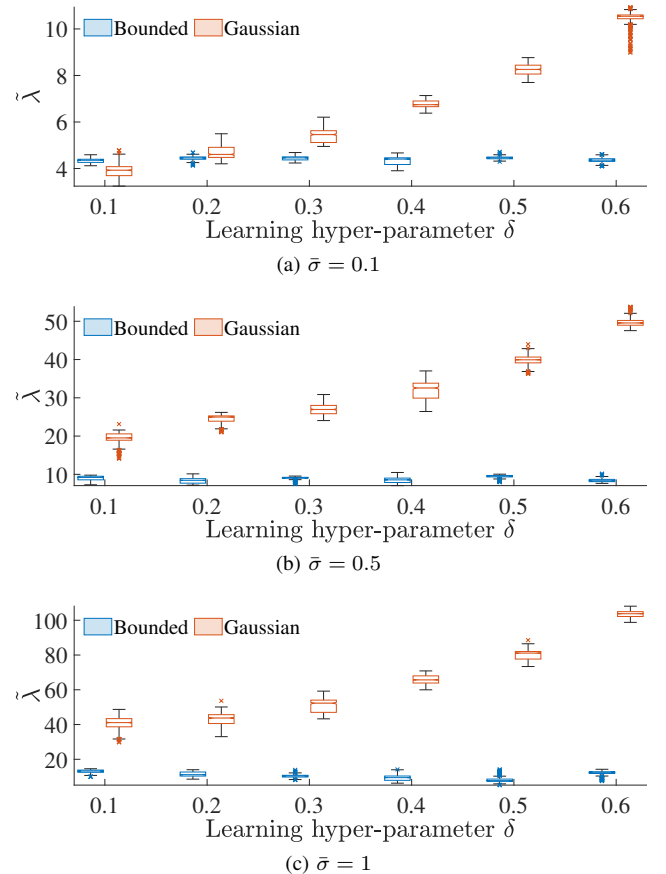


Fig. 2: Statistical results of 9000 times independent numerical experiments. The red box-plots are results for bounded disturbances with bound being $\bar{\phi} = n_x \sqrt{\bar{\sigma}}$, and the blue box-plots are results for Gaussian disturbances with covariance matrix being $\sigma_w = \bar{\sigma} I_{n_x}$.

recall that, if $(A_*, B_*) \in \Gamma(\Psi(n(k), \delta), \mathcal{D}(k))$, the following inequality holds:

$$Z(A_*, B_*)\Psi(n(k), \delta)Z^T(A_*, B_*) \succeq 0 \quad (83)$$

$$\Rightarrow \lambda_{n_x}(Z(A_*, B_*)\Psi(n(k), \delta)Z^T(A_*, B_*)) > 0, \quad (84)$$

where $\lambda_{n_x}(\cdot)$ denotes the minimum eigenvalue of a matrix. To validate this relationship, box plots [64] of the minimum eigenvalues $\tilde{\lambda} := \lambda_{n_x}(Z(A_*, B_*)\Psi(n(k), \delta)Z^T(A_*, B_*))$ are shown in Fig. 2, which indicates that the minimum eigenvalue of the matrix $Z(A_*, B_*)\Psi(n(k), \delta)Z^T(A_*, B_*)$ in each experiment is larger than zero. This result verifies the property of the proposed set-membership learning method (Theorem 1) because all the estimates satisfy

$$(A_*, B_*) \in \Gamma(\Psi(n(k), \delta), \mathcal{D}(k)). \quad (85)$$

Next, consider a linear time-invariant controllable system of the form (1) with A_* and B_* being

$$A_* = \begin{bmatrix} 0.850 & -0.038 & -0.038 \\ 0.735 & 0.815 & 1.594 \\ -0.664 & 0.697 & -0.064 \end{bmatrix}, \quad B_* = \begin{bmatrix} 1.431 & 0.705 \\ 1.620 & -1.129 \\ 0.913 & 0.369 \end{bmatrix}, \quad (86)$$

which is the example used in [12]. The disturbance \mathbf{w} is taken as an i.i.d. Gaussian disturbance with covariance matrix

being $\sigma_w = \text{diag}\{0.8, 0.8, 0.8\}$. This system is unstable since the eigenvalues of matrix A_* are $\{-0.7664, 0.8536, 1.5138\}$. The input signal u is designed to be a white disturbance before an ISC is obtained, and the state is initialized as $x(1) \sim \mathcal{N}(0, 5I)$. After determining an ISC according to (5)-(9), the proposed data-driven predictive controller is used to stabilize the system with parameters $\epsilon_l = 0.98$, $\delta = 0.3$, $\delta_1 = 0.8$, and

$$N = 5, \quad Q = \text{diag}\{5, 5, 5\}, \quad R = \text{diag}\{0.2, 0.2\}. \quad (87)$$

For every data sample $(x(k), u(k), x(k+1))$ in the dataset $\mathcal{D}(k+1)$, the ratio of the measures is defined as

$$\tilde{\epsilon}_l := \frac{\mathfrak{V}(\Gamma(\Psi(n(k)) + 1, \delta), \mathcal{D}(k+1)))}{\mathfrak{V}(\Gamma(\Psi(n(k), \delta), \mathcal{D}(k)))}. \quad (88)$$

By performing 1000 times of independent experiments, the histogram of $\tilde{\epsilon}_l$ is shown in Fig. 3, which shows that the inequality $\tilde{\epsilon}_l \leq \epsilon_l$ holds. Thus, in each experiment, the Lebesgue measure of the learned uncertainty set decreases exponentially, which verifies Theorem 2.

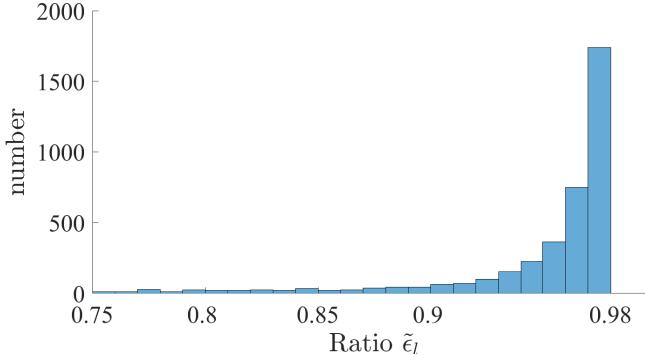


Fig. 3: Histogram of the ratio $\tilde{\epsilon}_l$ between the Lebesgue measures before and after a data sample is selected by the proposed ITL approach.

B. Comparative simulations

In this section, the proposed ETL protocol and data-driven predictive control method are compared with other data-driven controllers, including the DeePC proposed in [27] and RRL proposed in [10]. To do this, the system in (86) is still used. To ensure a fair performance comparison, the objective function of DeePC and RRL are set to be the same as that of the proposed controller with ITL according to (64), with matrices Q and R together with the control horizon N selected according to (87), and the input and state constraints are set to the same for all three controllers. The regularization weight parameters for DeePC are set to $\lambda_g = 30$, $\lambda_y = 10^5$ according to [27], and the length of epochs is set to be the same as the control horizon $N = 5$ for RRL according to [10]. To evaluate the control performance, we define the following weighted square error J_W as

$$J_W = \sum_{k=6}^{100} \mathbf{x}^T(k) Q \mathbf{x}(k) + \mathbf{u}^T(k) R \mathbf{u}(k). \quad (89)$$

The cost is calculated by summing stage costs at time instants $\{6, \dots, 100\}$ since data samples at times instants $\{1, \dots, 5\}$ are used to initialize the ISC.

Other metrics are also used for comparison, including the mean square error (MSE) of the states, the number of open-loop data points required to initiate the predictive controller¹ ($n(\bar{k}_0)$), the number of data points used to update the prediction model during closed-loop control ($n(100)$), and the total simulation time (which reflects the computation time used to execute the predictive controllers).

The state trajectories of different controllers are plotted in Fig. 4, and the comparison of the performance metrics is provided in Tab. I. By observing the comparison results in Fig. 4 and Tab. I, the proposed min-max predictive control method with the ITL protocol has a reduced computation time compared to DeePC and RRL methods. Compared to DeePC, the proposed approach requires fewer data to enable the initial design of the predictive control (measured by $n(k_0)$). This is because the number of the required data is influenced by the prediction length N in DeePC (see Theorem 5.1 in [27] for more details). Compared to RRL, the proposed ITL-based predictive control does not need to update the prediction model frequently (measured by $n(100)$). We also note that the computation complexity of finding a stabilizing control gain increases with the number of utilized data samples, since the dimension of the matrices involved in the solving process increases with the number of utilized data samples. From the simulation results shown in Fig. 4 and Table. I, the proposed ITL approach reduces the update frequency of the dataset, and thus further reduces the computational complexity.

In the ITL-based predictive control, the MSE and cost J_W are slightly larger than other approaches. Specifically, the MSE of ITL-based predictive control is 8.19% and 11% higher than DeePC and RRL, respectively, and the cost J_W of ITL-based predictive control is 8.04% and 12.45% higher than DeePC and RRL respectively. This gap is due to the fact that the proposed approach is a robust framework where the control sequence is mainly updated by considering the worst cases of disturbances and model uncertainties to achieve a trade-off between the robustness and the control performance.

TABLE I: Comparison of different performance metrics.

Method	DeePC [19]	RRL [8]	ITL
MSE	2.136	2.082	2.311
Cost J	5.708×10^3	5.484×10^3	6.167×10^3
$n(\bar{k}_0)$	23	6	5
$n(100)$	23	96	6
Simulation time	13.943s	20.109s	8.078s

C. Analysis of learning hyper-parameter δ

In this subsection, we analyze the impact of the learning hyper-parameter δ . To do this, the system parameters in (86) are used. The covariance matrix of the disturbance is set to

¹Here $n(\bar{k}_0)$ is consistent with the notation in Algorithm 1, but it is also abused to represent the number of the data points needed to initialize DeePC and RRL.

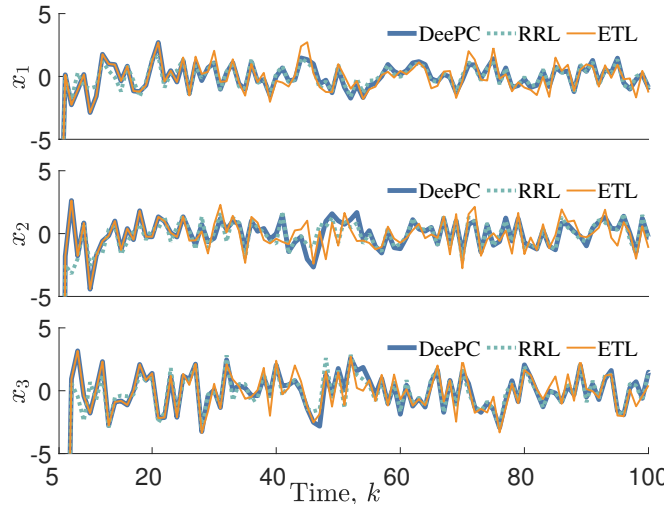


Fig. 4: Comparison of control performance between DeePC, RRL, and ITL-based predictive controllers.

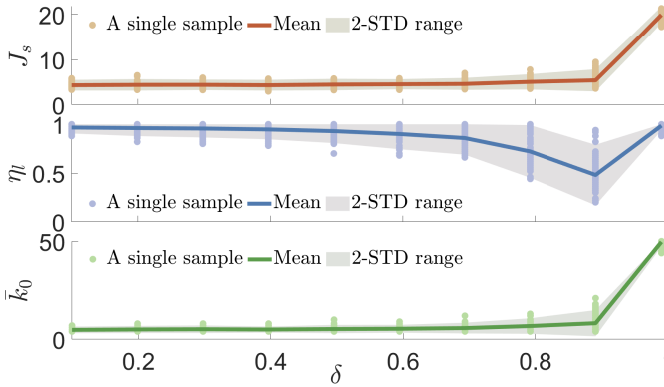


Fig. 5: Tradeoff analysis for ITL.

be $\sigma_w = \text{diag}\{0.12, 0.1, 0.08\}$, and other parameters are set to be the same to Section IV-A. The proposed controller with ITL is evaluated by choosing different values of δ , and the performance metrics are provided in Fig. 5, where \bar{k}_0 is the setup time used in Algorithm 1, the data rate η_l is defined as $\eta_l := \frac{n(50)}{50}$, and J_s is defined as

$$J_s := \log \left(\sum_{k=1}^{50} \mathbf{x}^T(k) Q \mathbf{x}(k) + \mathbf{u}^T(k) R \mathbf{u}(k) \right).$$

In Fig. 5, the solid lines represent the average values of 100-time tests. The single test results are marked with circles, and the shaded areas represent the ranges within two standard deviations from the expectation (namely, 2-STD range). From Fig. 5, the curves change slowly when $\delta \in (0, 0.6)$. The data rate η_l for $\delta \in (0, 0.6)$ stays high, since the parametric uncertainty set determined by (5) is relatively small and the effect of disturbances can easily trigger the learning condition. The setup time and mean square error when $\delta \in (0, 0.6)$ remain low because a smaller parametric uncertainty set $\Gamma(\Psi(n(k), \delta), \mathcal{D}(k))$ makes the existence of a stabilizing feedback gain easier. For $\delta \in (0.6, 0.9)$, the data rate η_l reduces rapidly; the reason is that in this range, a larger

δ strengthens the resistance of the set $\Gamma(\Psi(n(k), \delta), \mathcal{D}(k))$ against the disturbances. In Fig. 5, the curves corresponding to $\delta \in (0.9, 1)$ tend to diverge due to the potential nonexistence of an ISC. The reason is that a larger δ tolerates a larger set of possible parameters, making it difficult to find a feedback gain $K(k)$ that can stabilize all systems in $\Gamma(\Psi(n(k), \delta), \mathcal{D}(k))$. Based on the above analysis, the choice of parameter δ can be performed by compromising the trade-off between data efficiency and control performance; in practice, this can be done by taking into account the available computation power and prespecified performance requirements.

V. CONCLUSION

In this work, we consider a data-efficient learning problem for LTI systems subject to disturbances, and introduce an ITL approach which quantifies the innovation of the data samples online and updates the learned system dynamics only when an innovative data sample is identified. The estimate of the system dynamics is obtained with a set-membership learning approach, which is shown to be exponentially convergent with the increase of the number of the data points selected by ITL. We also show that the ITL can be integrated with data-driven predictive control, through utilizing a min-max optimization framework. In our next step, the extension of the proposed results to certain nonlinear dynamic systems will be further explored.

ACKNOWLEDGMENT

The authors would like to thank the Associate Editor and the anonymous reviewers for their suggestions which have improved the quality of the work.

REFERENCES

- [1] M. Tanaskovic, L. Fagiano, C. Novara, and M. Morari, "Data-driven control of nonlinear systems: An on-line direct approach," *Automatica*, vol. 75, pp. 1–10, 2017.
- [2] C. De Persis and P. Tesi, "Formulas for data-driven control: stabilization, optimality, and robustness," *IEEE Transactions on Automatic Control*, vol. 65, no. 3, pp. 909–924, 2019.
- [3] H. J. Van Waarde, J. Eising, H. L. Trentelman, and M. K. Camlibel, "Data informativity: a new perspective on data-driven analysis and control," *IEEE Transactions on Automatic Control*, vol. 65, no. 11, pp. 4753–4768, 2020.
- [4] J. Woo, S. Shin, A. T. Asutosh, J. Li, and C. J. Kibert, "An overview of state-of-the-art technologies for data-driven construction," in *Proceedings of the 18th International Conference on Computing in Civil and Building Engineering: ICCBE 2020*, pp. 1323–1334, Springer, 2021.
- [5] W. Tang and P. Daoutidis, "Data-driven control: Overview and perspectives," in *2022 American Control Conference (ACC)*, pp. 1048–1064, IEEE, 2022.
- [6] I. Markovsky, L. Huang, and F. Dörfler, "Data-driven control based on the behavioral approach: From theory to applications in power systems," *IEEE Control Systems Magazine*, vol. 43, no. 5, pp. 28–68, 2023.
- [7] F. Scheppe, "Recursive state estimation: Unknown but bounded errors and system inputs," *IEEE Transactions on Automatic Control*, vol. 13, no. 1, pp. 22–28, 1968.
- [8] M. Milanese and C. Novara, "Set membership identification of nonlinear systems," *Automatica*, vol. 40, no. 6, pp. 957–975, 2004.
- [9] M. Milanese, J. Norton, H. Piet-Lahanier, and É. Walter, *Bounding approaches to system identification*. Springer Science & Business Media, 2013.
- [10] J. Umenberger, M. Ferizbegovic, T. B. Schön, and H. Hjalmarsson, "Robust exploration in linear quadratic reinforcement learning," *Advances in Neural Information Processing Systems*, vol. 32, 2019.

[11] S. Dean, H. Mania, N. Matni, B. Recht, and S. Tu, "On the sample complexity of the linear quadratic regulator," *Foundations of Computational Mathematics*, vol. 20, no. 4, pp. 633–679, 2020.

[12] H. J. van Waarde, M. K. Camlibel, and M. Mesbahi, "From noisy data to feedback controllers: Nonconservative design via a matrix S-lemma," *IEEE Transactions on Automatic Control*, vol. 67, no. 1, pp. 162–175, 2020.

[13] M. Milanese and C. Novara, "Model quality in identification of nonlinear systems," *IEEE Transactions on Automatic Control*, vol. 50, no. 10, pp. 1606–1611, 2005.

[14] C. Novara, "Sparse identification of nonlinear functions and parametric set membership optimality analysis," *IEEE Transactions on automatic control*, vol. 57, no. 12, pp. 3236–3241, 2012.

[15] M. Karimshoushtari and C. Novara, "Design of experiments for nonlinear system identification: A set membership approach," *Automatica*, vol. 119, p. 109036, 2020.

[16] M. Milanese and M. Taragna, " H_∞ set membership identification: A survey," *Automatica*, vol. 41, no. 12, pp. 2019–2032, 2005.

[17] N. Ozay, C. Lagoa, and M. Sznajer, "Set membership identification of switched linear systems with known number of subsystems," *Automatica*, vol. 51, pp. 180–191, 2015.

[18] M. Lauricella and L. Fagiano, "Set membership identification of linear systems with guaranteed simulation accuracy," *IEEE Transactions on Automatic Control*, vol. 65, no. 12, pp. 5189–5204, 2020.

[19] E. Aggelogiannaki and H. Sarimveis, "Nonlinear model predictive control for distributed parameter systems using data driven artificial neural network models," *Computers & Chemical Engineering*, vol. 32, no. 6, pp. 1225–1237, 2008.

[20] A. Chakrabarty, G. T. Buzzard, and S. H. Žak, "Output-tracking quantized explicit nonlinear model predictive control using multiclass support vector machines," *IEEE Transactions on Industrial Electronics*, vol. 64, no. 5, pp. 4130–4138, 2016.

[21] U. Rosolia, X. Zhang, and F. Borrelli, "Data-driven predictive control for autonomous systems," *Annual Review of Control, Robotics, and Autonomous Systems*, vol. 1, pp. 259–286, 2018.

[22] R. Iglesias, F. Rossi, K. Wang, D. Hallac, J. Leskovec, and M. Pavone, "Data-driven model predictive control of autonomous mobility-on-demand systems," in *2018 IEEE international conference on robotics and automation (ICRA)*, pp. 6019–6025, IEEE, 2018.

[23] M. Korda and I. Mezić, "Linear predictors for nonlinear dynamical systems: Koopman operator meets model predictive control," *Automatica*, vol. 93, pp. 149–160, 2018.

[24] D. Bruder, X. Fu, R. B. Gillespie, C. D. Remy, and R. Vasudevan, "Data-driven control of soft robots using Koopman operator theory," *IEEE Transactions on Robotics*, vol. 37, no. 3, pp. 948–961, 2020.

[25] P. Verheijen, V. Breschi, and M. Lazar, "Handbook of linear data-driven predictive control: Theory, implementation and design," *Annual Reviews in Control*, vol. 56, p. 100914, 2023.

[26] J. C. Willems, P. Rapisarda, I. Markovsky, and B. L. De Moor, "A note on persistency of excitation," *Systems & Control Letters*, vol. 54, no. 4, pp. 325–329, 2005.

[27] J. Coulson, J. Lygeros, and F. Dörfler, "Data-enabled predictive control: In the shallows of the DeePC," in *2019 18th European Control Conference (ECC)*, pp. 307–312, IEEE, 2019.

[28] J. Coulson, J. Lygeros, and F. Dörfler, "Regularized and distributionally robust data-enabled predictive control," in *2019 IEEE 58th Conference on Decision and Control (CDC)*, pp. 2696–2701, IEEE, 2019.

[29] J. Coulson, J. Lygeros, and F. Dörfler, "Distributionally robust chance constrained data-enabled predictive control," *IEEE Transactions on Automatic Control*, vol. 67, no. 7, pp. 3289–3304, 2021.

[30] E. Elokda, J. Coulson, P. N. Beuchat, J. Lygeros, and F. Dörfler, "Data-enabled predictive control for quadcopters," *International Journal of Robust and Nonlinear Control*, vol. 31, no. 18, pp. 8916–8936, 2021.

[31] L. Huang, J. Lygeros, and F. Dörfler, "Robust and kernelized data-enabled predictive control for nonlinear systems," *IEEE Transactions on Control Systems Technology*, 2023.

[32] S. Baros, C.-Y. Chang, G. E. Colon-Reyes, and A. Bernstein, "Online data-enabled predictive control," *Automatica*, vol. 138, p. 109926, 2022.

[33] L. Schmitt, J. Beerwerth, M. Bahr, and D. Abel, "Data-driven predictive control with online adaption: Application to a fuel cell system," *IEEE Transactions on Control Systems Technology*, 2023.

[34] L. Hewing, J. Kabzan, and M. N. Zeilinger, "Cautious model predictive control using Gaussian process regression," *IEEE Transactions on Control Systems Technology*, vol. 28, no. 6, pp. 2736–2743, 2019.

[35] E. Bradford, L. Imsland, D. Zhang, and E. A. del Rio Chanona, "Stochastic data-driven model predictive control using Gaussian processes," *Computers & Chemical Engineering*, vol. 139, p. 106844, 2020.

[36] M. Tanaskovic, L. Fagiano, R. Smith, and M. Morari, "Adaptive receding horizon control for constrained MIMO systems," *Automatica*, vol. 50, no. 12, pp. 3019–3029, 2014.

[37] M. Lorenzen, M. Cannon, and F. Allgöwer, "Robust MPC with recursive model update," *Automatica*, vol. 103, pp. 461–471, 2019.

[38] J. Umlauf, T. Beckers, A. Capone, A. Lederer, and S. Hirche, "Smart forgetting for safe online learning with Gaussian processes," in *Proceedings of the 2nd Conference on Learning for Dynamics and Control*, vol. 120, (Zürich, Switzerland), 2020.

[39] H. Schluter, F. Solowjow, and S. Trimpe, "Event-triggered learning for linear quadratic control," *IEEE Transactions on Automatic Control*, pp. 4485–4498, 2020.

[40] K. He, Y. Deng, G. Wang, X. Sun, Y. Sun, and Z. Chen, "Learning-based trajectory tracking and balance control for bicycle robots with a pendulum: A Gaussian process approach," *IEEE/ASME Transactions on Mechatronics*, vol. 27, no. 2, pp. 634–644, 2022.

[41] K. Zheng, D. Shi, Y. Shi, and J. Wang, "Non-parametric event-triggered learning with applications to adaptive model predictive control," *IEEE Transactions on Automatic Control*, 2022.

[42] J. Umlauf and S. Hirche, "Feedback linearization based on Gaussian processes with event-triggered online learning," *IEEE Transactions on Automatic Control*, vol. 65, no. 10, pp. 4154–4169, 2019.

[43] A. Lederer, A. J. O. Conejo, K. A. Maier, W. Xiao, J. Umlauf, and S. Hirche, "Gaussian process-based real-time learning for safety critical applications," in *International Conference on Machine Learning*, pp. 6055–6064, PMLR, 2021.

[44] J. Jiao, A. Capone, and S. Hirche, "Backstepping tracking control using Gaussian processes with event-triggered online learning," *IEEE Control Systems Letters*, vol. 6, pp. 3176–3181, 2022.

[45] J. Beuchert, F. Solowjow, J. Raisch, S. Trimpe, and T. Seel, "Hierarchical event-triggered learning for cyclically excited systems with application to wireless sensor networks," *IEEE Control Systems Letters*, vol. 4, no. 1, pp. 103–108, 2020.

[46] J.-D. Diao, J. Guo, and C.-Y. Sun, "Event-triggered identification of FIR systems with binary-valued output observations," *Automatica*, vol. 98, pp. 95–102, 2018.

[47] J. Guo and J.-D. Diao, "Prediction-based event-triggered identification of quantized input FIR systems with quantized output observations," *Science China Information Sciences*, vol. 63, no. 1, pp. 1–12, 2020.

[48] D. Piga, S. Formentini, and A. Bemporad, "Direct data-driven control of constrained systems," *IEEE Transactions on Control Systems Technology*, vol. 26, no. 4, pp. 1422–1429, 2017.

[49] I. Abraham and T. D. Murphey, "Active learning of dynamics for data-driven control using Koopman operators," *IEEE Transactions on Robotics*, vol. 35, no. 5, pp. 1071–1083, 2019.

[50] G. Baggio, D. S. Bassett, and F. Pasqualetti, "Data-driven control of complex networks," *Nature communications*, vol. 12, no. 1, p. 1429, 2021.

[51] B. D. Anderson and J. B. Moore, *Optimal filtering*. Prentice-Hall, Inc, 1979.

[52] L. Ljung, *System Identification: Theory for the User*. Pearson, 1998.

[53] R. A. Horn and C. R. Johnson, *Matrix analysis*. Cambridge university press, 2012.

[54] K. Alexander and V. Istvan, *Ellipsoidal Calculus for Estimation and Control*, vol. 1. Birkhäuser Boston, MA, 1997.

[55] H. J. van Waarde, M. K. Camlibel, J. Eising, and H. L. Trentelman, "Quadratic matrix inequalities with applications to data-based control," *SIAM Journal on Control and Optimization*, vol. 61, no. 4, pp. 2251–2281, 2023.

[56] T. Brailovskaya and R. van Handel, "Universality and sharp matrix concentration inequalities," *arXiv preprint arXiv:2201.05142*, 2022.

[57] R. Ahlswede and A. Winter, "Strong converse for identification via quantum channels," *IEEE Transactions on Information Theory*, vol. 48, no. 3, pp. 569–579, 2002.

[58] K. Pelckmans, J. De Brabanter, J. A. Suykens, and B. De Moor, "The differogram: Non-parametric noise variance estimation and its use for model selection," *Neurocomputing*, vol. 69, no. 1, pp. 100–122, 2005.

[59] J. A. Rossiter, B. Kouvaritakis, and M. Rice, "A numerically robust state-space approach to stable-predictive control strategies," *Automatica*, vol. 34, no. 1, pp. 65–73, 1998.

[60] D. Mayne, "Robust and stochastic MPC: are we going in the right direction?," *IFAC-PapersOnLine*, vol. 48, no. 23, pp. 1–8, 2015.

[61] F. A. Bayer, F. D. Brunner, M. Lazar, M. Wijnand, and F. Allgöwer, "A tube-based approach to nonlinear explicit MPC," in *2016 IEEE 55th Conference on Decision and Control (CDC)*, pp. 4059–4064, IEEE, 2016.

- [62] R. D. McAllister and J. B. Rawlings, "The stochastic robustness of nominal and stochastic model predictive control," *IEEE Transactions on Automatic Control*, pp. 1–13, 2022.
- [63] J. B. Rawlings, D. Q. Mayne, and M. M. Diehl, *Model predictive control: theory, computation, and design 2nd edition*. Nob Hill Publishing, LLC, 2019.
- [64] E. O'Dwyer, E. C. Kerrigan, P. Falugi, M. Zagorowska, and N. Shah, "Data-driven predictive control with improved performance using segmented trajectories," *IEEE Transactions on Control Systems Technology*, vol. 31, no. 3, pp. 1355–1365, 2023.



Kaikai Zheng was born in Xianyang, Shaanxi Province, China. He received the B.Eng. degree in automation from Beijing Institute of Technology, Beijing, China, in 2020. He is taking successive postgraduate and doctoral programs at the School of Automation, Beijing Institute of Technology. His research interests include event-based state estimation, system identification, event-triggered learning, and model predictive control.



as a Postdoctoral Fellow in bioengineering. Since July 2018, he has been with the School of Automation, Beijing Institute of Technology, where he is a professor.

His research focuses on the analysis and synthesis of complex sampled-data control systems with applications to biomedical engineering, robotics, and motion systems. He serves as an Associate Editor/Technical Editor for *IEEE Transactions on Industrial Electronics*, *IEEE/ASME Transactions on Mechatronics*, *IEEE Control Systems Letters*, and *IET Control Theory and Applications*. He is a member of the Early Career Advisory Board of Control Engineering Practice. He was a Guest Editor for *European Journal of Control*. He served as an associate editor for *IFAC World Congress* and is a member of the *IEEE Control Systems Society Conference Editorial Board*. He is a Senior Member of the IEEE.



Yang Shi received the Ph.D. degree in electrical and computer engineering from the University of Alberta, Edmonton, AB, Canada, in 2005. From 2005 to 2009, he was an Assistant Professor and an Associate Professor in the Department of Mechanical Engineering, University of Saskatchewan, Saskatoon, SK, Canada. In 2009, he joined the University of Victoria, Victoria, BC, Canada, where he is currently a Professor in the Department of Mechanical Engineering. His current research interests include networked and distributed systems, model predictive control (MPC), cyber-physical systems (CPS), robotics and mechatronics, navigation and control of autonomous systems (AUV and UAV), and energy system applications.

Dr. Shi received the University of Saskatchewan Student Union Teaching Excellence Award in 2007, and the Faculty of Engineering Teaching Excellence Award in 2012 at the University of Victoria (UVic). He is the recipient of the JSPS Invitation Fellowship (short-term) in 2013, the UVic Craigdarroch Silver Medal for Excellence in Research in 2015, the 2016 *IEEE Transactions on Fuzzy Systems Outstanding Paper Award*, the Humboldt Research Fellowship for Experienced Researchers in 2018. He is Vice-President on Conference Activities of IEEE IES, and Chair of IES Technical Committee of Industrial Cyber-Physical Systems. Currently, he is Co-Editor-in-Chief for *IEEE Transactions on Industrial Electronics*; he also serves as Associate Editor for *Automatica*, *IEEE Transactions on Automatic Control*, *IEEE Transactions on Cybernetics*, etc. He is General Chair of the 2019 International Symposium on Industrial Electronics (ISIE) and the 2021 International Conference on Industrial Cyber-Physical Systems (ICPS). He is a Fellow of IEEE, ASME, Engineering Institute of Canada (EIC), and Canadian Society for Mechanical Engineering (CSME), and a registered Professional Engineer in British Columbia, Canada.



Sandra Hirche received the Diplom-Ingenieur degree in aeronautical engineering from Technical University Berlin, Berlin, Germany, in 2002, and the Doktor-Ingenieur degree in electrical engineering from Technical University Munich, Munich, Germany, in 2005.

From 2005 to 2007, she was awarded a Post-Doctoral Scholarship from the Japanese Society for the Promotion of Science, Fujita Laboratory, Tokyo Institute of Technology, Tokyo, Japan. From 2008 to 2012, she has been an

Associate Professor with the Technical University of Munich. She has been a TUM Liesel Beckmann Distinguished Professor since 2013 and heads the Chair of Information-Oriented Control with the Department of Electrical and Computer Engineering Technical University Munich. She has authored or coauthored more than 150 articles in international journals, books, and refereed conferences. Her main research interests include cooperative, distributed and networked control with applications in human-robot interaction, multirobot systems, and general robotics.